Carbohydrate Polymers 84 (2011) 1019–1026

Contents lists available at ScienceDirect

Carbohydrate Polymers

journal homepage: www.elsevier.com/locate/carbpol

Isolation and characterization of exopolysaccharides from seaweed associated bacteria *Bacillus licheniformis*

Ravindra Pal Singh, Mahendra K. Shukla, Avinash Mishra, Puja Kumari, C.R.K. Reddy*, Bhavanath Jha

Discipline of Marine Biotechnology and Ecology, Central Salt and Marine Chemicals Research Institute, Council of Scientific and Industrial Research (CSIR), Bhavnagar 364021, India

ARTICLE INFO

Article history:
Received 2 December 2010
Received in revised form
17 December 2010
Accepted 19 December 2010
Available online 25 December 2010

Keywords:
Exopolysaccharide
MALDI-TOF-TOF MS
Bacillus licheniformis
Seaweed
Atomic force microscopy
X-ray diffraction

ABSTRACT

In the present study, EPS secreted by the endophytic bacterium *Bacillus licheniformis* was isolated and characterized. The molecular masses of the EPS were 1540 and 44,565 kDa and ^{1}H NMR, FT-IR and UV–Vis spectral analyses revealed prevalence of characteristic primary amine-group, aromatic-compound, halide and aliphatic alkyl-group in addition to Na, P, Ca, C, O, Cl and S as inferred from EDX analysis. XRD and DSC analysis confirmed the amorphous nature of EPS, showing an average particle size of 24.977 μm (*d* 0.5) with 191 nm average roughness. The positive ion reflector mode of MALDI TOF-TOF MS exhibited a series of low and high mass peaks corresponding to various oligosaccharides and polysaccharides respectively. Further, GC–MS analysis revealed its four monosaccharide constituents glucose, galactose, mannose and arabinose. The potential heterogeneous properties of EPS as revealed in the present study may be explored in various biotechnological and industrial applications.

1. Introduction

Microbial exopolysaccharides (EPSs) are biosynthetic polymers mainly consisting of carbohydrates secreted by bacteria (Freitas et al., 2009) and cyanobacteria (Chi, Su, & Lu, 2007; Decho, 1990; Parikh & Madamwar, 2006), however, it is also reported from Cryptophyta (Bermudez, Rosales, Loreto, Briceno, & Morales, 2004), mushroom (Zou, Sun, & Guo, 2006), yeast (Duan, Chi, Wang, & Wang, 2008) and basidiomycetes (Chi & Zhao, 2003; Manzoni & Rollini, 2001). EPSs constitute different classes of organic macromolecules such as polysaccharides, proteins, nucleic acids, phospholipids and other polymeric compounds thereby carrying different organic functional groups such as acetyl, succinyl or pyruvyl and some inorganic constituent like sulfate (Nielsen & Jahn, 1999). Depending on their location, EPSs occur in two forms either in capsular (polymers being closely associated with the cell surface) or slimy polysaccharides (loosely associated with the cell surface) (Costerton, 1999).

In recent years, interest in the exploitation of valuable EPSs has been considerably increased towards polysaccharide producing bacteria and cyanobacteria for various industrial applications (Mishra & Jha, 2009). The EPSs produced by marine bacteria have been utilized as ingredients in food products, pharmacy, petroleum industry and emulsification of crude oil, hydrocarbons, vegetable, mineral oils and bioremediation agents in environment management system (Costerton, 1999; Jia, Yu, Lin, & Dai, 2007). Apart from these, they have also been implicated in biofilm formation in marine ecosystem thereby enhancing the survival of microbes under abiotic and biotic stress by influencing their physicochemical environment (Bhaskar & Bhosle, 2005; Duan et al., 2008).

The bacteria are ubiquitous colonizers on the surface of seaweed and are reported to play important roles in their growth, development and reproduction (Marshall, Joint, Callow, & Callow, 2006). Similar findings have been demonstrated with *Bacillus licheniformis* which influence the life history and developmental morphology of *Ulva fasciata* (Singh, Mantri, Reddy, & Jha, 2011) in corresponding to increase the zoospore production and in attaining the normal foliose morphology. Further, seaweed–bacteria interactions are partly attributed to the extracellular substances secreted by associated marine bacteria. The previous reports reveal that the addition of supernatants of morphogenesis-inducing bacterial isolates were capable of giving the same effect (Marshall et al., 2006; Tatewaki, Provasoli, & Pintner, 1983).

In this study, an attempt was made to extract and characterize the chemical and physical properties of EPS produced by an endophytic bacterium *B. licheniformis* associated with *Gracilaria dura* with the help of advanced analytical techniques. Despite the biotechnological potential of these biopolymers from marine and estuarine environments, the role of EPS in seaweed–bacteria inter-

* Corresponding author. Tel.: +91 278 256 5801/256 3805x614; fax: +91 278 256 6970/256 7562.
E-mail address: crk@csmcri.org (C.R.K. Reddy).

0144-8617/$ – see front matter © 2010 Elsevier Ltd. All rights reserved.
doi:10.1016/j.carbpol.2010.12.061

action remains largely untapped. Thus, the EPS produced from seaweed associated bacterium in the pure liquid cultures were characterized to unravel its constituents that may increase our understanding of the seaweed–bacterial association in the marine environment further.

2. Material and methods

2.1. Growth curve and exopolysaccharides production

An endophytic bacterium *B. licheniformis* (NCBI accession number GU723480) was isolated from *G. dura*. A batch culture with isolated marine bacteria was maintained for EPSs production in 200 ml of nutrient broth supplemented with 3.5% NaCl (w/v) and 0.02% (w/v) glucose in Erlenmeyer flasks on a rotary shaker (160 g) at 30 ± 2 °C for 3 days. The pH of the medium was adjusted to 7.0 with 1 N NaOH. Sub samples of 5 ml aliquots were drawn at regular intervals for bacterial growth (A_{600} nm). Bacterial cells were harvested in stationary phase by centrifuging the culture medium at 15,000 × *g*, 4 °C for 30 min. The cell pellets were freeze-dried and weighed. The supernatants were pressure-filtered through cellulose nitrate filters with 0.45 and 0.25 μm pore size (Millipore filters, Bangalore, India). EPS was precipitated from the final filtrate after the addition of three volumes of cold isopropanol and solution was kept overnight at 4 °C. The resulting precipitate was recovered by vacuum filtration through a sintered glass apparatus. An additional 100 ml of cold isopropanol was added and solution was kept at −20 °C overnight for precipitation. The precipitates were washed with 70–100% ethanol–water mixtures followed by ethanol. Thereafter, EPS was collected, dried and stored at room temperature. They were redissolved in distilled water and dialyzed at 4 °C for 24 h against distilled water for desalting. Excess water was removed under vacuum and lyophilized EPS was stored at room temperature until chemical and physical analyses were performed. For chemical analyses, lyophilized EPS was hydrolyzed with 2 N HCl for 2 h at 100 °C in ampoules flushed with N_2 before sealing and thereafter the solution was evaporated to dryness under reduced pressure at 40 °C (Rougeaux, Talaga, Carlson, & Guezennec, 1998).

2.2. Emulsifying activity

The emulsifying activity of EPS was determined according to Nielsen and Jahn (1999) method modified by Bramhachari et al. (2007). Briefly, lyophilized EPS (0.5 mg) was dissolved in 0.5 ml deionized water and volume was made up to 2 ml using phosphate-buffered saline (PBS). The sample mixture were vigorously vortexed for 1 min after the addition of different hydrophobic substrates (petrol, xylene, toluene, Tween-80, ground nut and mineral oils). Samples were incubated at 30 °C with a reciprocal shaking speed of 60 × *g* and absorbance was read immediately before and after vortexing (A_0) at 540 nm. The decrease in absorbance was recorded after incubation at room temperature for 30 and 60 min (A_t). A control was run simultaneously with 2 ml of PBS and 0.5 ml of hexadecane without EPS. The emulsification activity was expressed as the percentage retention of emulsion during incubation for time, *t*: $A_t/A_0 \times 100$ (Bramhachari et al., 2007).

2.3. Purification and determination of molecular weight

The crude EPS was purified by Sephadex G-50 (2.5 cm × 50 cm) with ratio of H_2O/pyridine/acetic acid (500/5/2, V/V/V) and eluted with 5 ml fractions collected at a flow rate of 5 ml h^{-1}. The fractions were then subjected to anion-exchange chromatography (DEAE-Sepharose CL-6B; 1.5 cm × 40 cm) and eluted (10 ml fractions) with 0.1 l of H_2O and 1 l of NaCl gradient from 0 to 1 M at a flow rate of 10 ml h^{-1}. The isolated fractions were measured by the phenol–sulphuric acid method (absorbance was taken at 490 nm). The EPSs fractions were lyophilized and utilized for further characterization.

The molecular weight of sample was determined by gas permeation chromatography (GPC, Water Allaince, model 2695). A measure of 50 μl (2% w/v) EPS was loaded to GPC column ultrahydrogel 120 and 500 at 40 °C and elution was monitored by a refractive index detector (2414). The column was calibrated with standard dextran (molecular weight; 5200–668,000 kDa) from PSS, USA.

2.4. Chemical analysis of exopolysaccharide

Lyophilized EPS (5 mg) was dissolved in 5 ml deionized water by heating at 80 °C for about 15–20 min and allowed to cool at room temperature (28 ± 2 °C). EPS was assayed for its total carbohydrate contents by following the anthrone method with glucose as standard (Yemm & Willis, 1954) and protein content was determined by Bradford method (Bradford, 1976) with BSA as standard. Sulfate was determined by Dodgson and Price (1963) method. Briefly, EPS was added to the precipitation solution (13.6% $BaCl_2 \cdot 2H_2O$ and 2.67% Tween-80), allowed to stand at room temperature for 30 min and absorbance was taken at 420 nm. The amount of sulfate was calculated using a standard curve established in the range of 2–20 μg ml^{-1} H_2SO_4. Further, the monosaccharide contents of EPS were estimated by alditol–acetate method (Siddhanta et al., 2001).

2.5. UV–Vis, FT-IR and ^{1}H NMR

The UV–visible spectrum of EPS was recorded between 200 and 800 nm on a spectrophotometer. Pellets of 0.75 mg of EPS were prepared with KBr followed by pressing the mixture into a 16 mm diameter mold. FT-IR spectrum was recorded on Perkin Elmer (Spectrum GX) with a resolution of 4 cm^{-1} in 4000–400 cm^{-1} region (Wang et al., 2004). Noise-decoupled ^{1}H NMR spectrum was recorded on a Bruker Avance-II 200 spectrometer, Switzerland, at 200 MHz. EPS of the *B. licheniformis* was dissolved in the d-NaOH (50 mg ml^{-1}) and spectra was recorded at 25 °C with 5000–5200 accumulations, pulse duration 5.9 μs, acquisition time 1.2 s and relaxation delay 6 μs.

2.6. Energy dispersive X-ray spectroscopy, particle size distribution and atomic force microscopy (AFM)

Elemental analysis of EPS was done using energy dispersive X-ray spectroscopy (EDS or EDX; Oxford Instruments, UK) and particle size distributions were measured by laser diffraction (Malvern Mastersizer 2000, Malvern Ltd., Worcestershire, UK). For AFM, the glass cover slips (Himedia, India) were treated with a mixture of 15 ml of HCl and 5 ml of HNO_3 for 30 min followed by treatment with a mixture of 20 ml of H_2SO_4 and 5 ml of H_2O_2 for 30 min. After rinsing the cover slip with Milli-Q water, stored in Milli-Q for later use. Samples for AFM were prepared according to Grabar, Freeman, Hommer, and Natan (1995). An AFM consists of a sharp tip, attached to a cantilever, which rasters over the surface of the sample in a bound scan area and the movement of the cantilever, as the tip moves across the surface, is recorded to produce the image of the sample. The image of the sample was taken in tapping mode of AFM.

2.7. X-ray diffraction (XRD) analysis

X-ray diffraction (XRD) was performed on X-ray powder diffractometer (Philips X'pert MPD, The Netherlands) instrument equipped with a PW3123/00 curved Ni-filtered CuKα (λ = 1.54056 Å) radiation generated at 40 kV and 30 mA with liquid nitrogen cooled solid-state germanium detector to study the

physical properties of EPS using slow scan in different ranges of two-theta angles (2–80°). The specimen length and irradiated length were 10 mm, with receiving slit size of 0.2 mm and 200 mm goniometer radius. The distance between focus and divergences slit were 100 mm. The dried EPS sample was mounted on a quartz substrate and intensity peaks of diffracted X-rays were continuously recorded with scan step time 1 s at 25 °C while *d*-spacings appropriate to diffracted X-rays at that value of θ was calculated with Bragg's law.

$$d = \frac{\lambda}{2 \sin \theta}$$

where θ is half of the scattering angle measured from the incident beam.

Crystallinity index (CI_{xrd}) was calculated from the area under crystalline peaks normalized with corresponding to total scattering area (Ricou, Pinel, & Juhasz, 2005).

$$CI_{xrd} = \frac{\sum A_{crystal}}{\sum A_{crystal} + \sum A_{amorphous}}$$

2.8. Thermal gravimetric analysis (TGA) and differential scanning calorimetric (DSC) analysis

TG and DSC analysis of EPS were carried with Mettler Toledo TGA/SDTA System (Greifensee, Switzerland). About 5 mg of dried sample was used for the TGA and DSC experiment. TGA and DSC thermograms were obtained in the range of 30–480 °C and 30–450 °C, respectively, under nitrogen atmosphere at rate of 10 °C min^{-1}. Their respective graphs were plotted with weight (percentage) loss and heat flow vs temperatures, respectively. The activation energy (Ea) was calculated with Arrhenius equation while enthalpy of transition (ΔH) and crystallinity of the EPS (CI_{DSC}) were calculated with the following equation (Khanna & Kuhn, 1997).

$$Ea = -2.303RT \log_{10} \frac{k}{A}$$

where R is the universal gas constant, A is the frequency factor for the reaction, T is the temperature (K, 298 °C) and k is the reaction rate coefficient. The value was calculated for the nth order of the reaction.

$$\Delta H_{total} = KA$$

where ΔH is the enthalpy of transition, K is the calorimetric constant and A is area under the curve.

$$CI_{DSC} = \frac{\Delta H_{Net}}{H_{total}}$$

where ΔH_{Net} is difference between heat of crystallization and melting.

2.9. MALDI (matrix assisted laser desorption–ionization) TOF-TOF mass spectroscopy

The EPS was dissolved in acetonitrile (5% w/v; 1 mg ml^{-1}), desalted and mixed with equal volume of matrix α-cyano-4-hydroxycinnamic acid (5 mg ml^{-1}). MALDI TOF-TOF MS analysis was performed on an Applied Biosystem 4800 MALDI TOF-TOF analyzer with an Nd-YAG (neodymium-doped yttrium aluminium garnet) laser (355 nm, 200 Hz) operated in accelerated voltage (20 kV). Each spectrum was collected in reflector mode (300 cm) as an average of 2000 laser shots per spectrum (Mishra, Kavita, & Jha, 2011). Reproducibility of the spectrum was checked from 12 spot-sets in each mode and spectra were analyzed after centroids and de-isotoping using data explorer software (Applied Biosystem, USA).

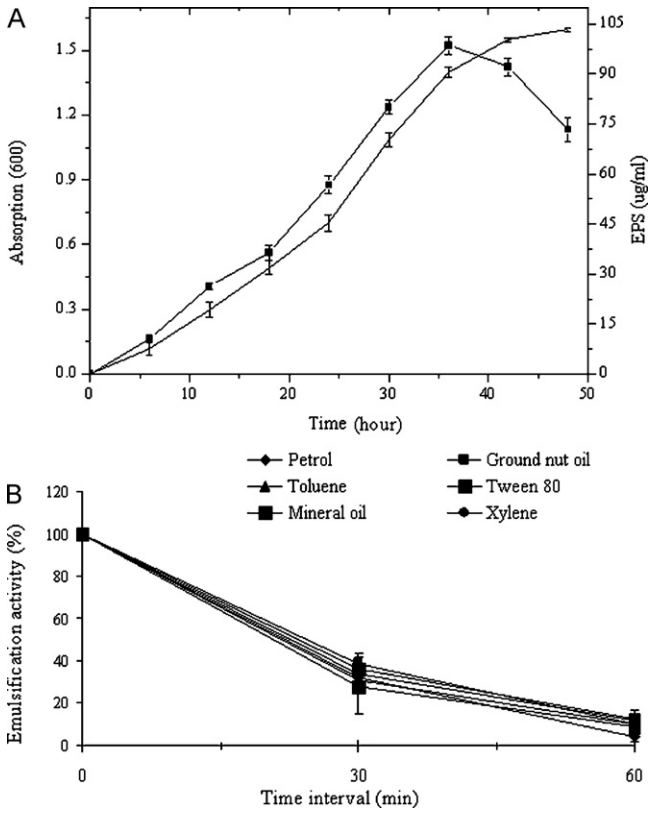

Fig. 1. Growth, EPSs production (A) and emulsifying activity (B) of *B. licheniformis*.

3. Results and discussion

3.1. Optimization of EPS production

The slimy EPS content varied with time interval and was maximal during the late log phase of bacterial growth. The *B. licheniformis* showed maximum production of EPS with 576 mg l^{-1} dry cell weight after three days. The EPS yield in batch culture varied with incubation period and ranged from 11.5 μg ml^{-1} dry cell weight to 60.2 μg ml^{-1} dry cell weight at 6 h and 24 h, respectively (Fig. 1A). The EPS content reported in the present study was substantially higher than previously reported values (138.6 mg l^{-1}) for other *Bacillus* sp. (Maugeri et al., 2002).

3.2. Emulsifying activity

The emulsification property of EPS was determined by its strength to retain the emulsion breaks rapidly within an initial incubation of 30 and 60 min (Fig. 1B). The dialyzed fraction of the exopolymer produced by *B. licheniformis* retained 32.14% and 3.9% in petrol, 38.43% and 10.2% in ground nut oil, 30.88% and 10.29% in toluene, 28.12% and 8.68% in mineral oil, 36.25% and 12.64% in Tween-80 and 33.94% and 11.67% in xylene of the emulsification activity after 30 min and 60 min, respectively. Among different oils investigated, petrol was the most effectively emulsified by EPS of *B. licheniformis* and was higher than earlier reports (Bramhachari et al., 2007). This EPS was also capable of emulsifying hydrocarbons at a percentage higher than the control. The functional groups in the molecular chains of the polymer are considered as important determinants for emulsification activity. The emulsions produced by the polysaccharides from *B. licheniformis* were stable and composed

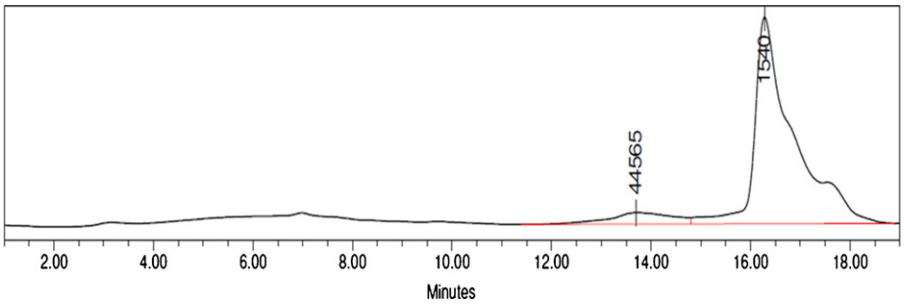

Fig. 2. GPC representation molecular weight of EPSs of *B. licheniformis*.

of small, uniform droplets with fine and smooth consistency. This makes them a lucrative emulsifying agents that can be explored in food and oil industries, where emulsifiers from microbial sources are exploited owing to their advantages against synthetic products, such as lower toxicity, higher biodegradability and better environmental compatibility (extreme temperature, pH and salinity) (Bermudez et al., 2004).

3.3. Purification and determination of molecular mass

A single peak was obtained with 0.4 mol l^{-1} of NaCl concentration after DEAE-Sepharose CL-6B column for EPS produced by *B. licheniformis* (Fig. S1). The bacterial EPSs generally consist of single and/or double fractions with molecular masses between 20 and 2000 kDa (Arias et al., 2003; Manzoni & Rollini, 2001). However, high molecular masses are also reported for EPSs produced by *Idiomarina* spp. (1.5×10^4–1.5×10^6), *Alteromonas hispanica* (1.9×10^7) and even *Bacillus* strain B3-15 (6×10^5) (Manzoni & Rollini, 2001; Mata et al., 2006). The GPC chromatogram of the purified EPS in the present study generated two peaks corresponding to fractions, 1540 and 44,565 kDa approximately with 1.92 and 1.41 polydispersity, respectively (Fig. 2 and Table S1).

3.4. Chemical analysis

The contents of total carbohydrates, protein and sulfate were found to be 343.14, 107.68 and 50.28 mg l^{-1}, respectively in EPS produced by *B. licheniformis*. In general, carbohydrate contents of the EPSs were higher than sulfate and proteins, a feature that has also been observed with other bacterial EPSs (Zhenming & Yan, 2005). Further, GC–MS analysis confirmed the presence of glucose (54.38%), mannose (25.24%), galactose (11.32%) and arabinose (9.06%) components of carbohydrate fraction (Fig. S2). To our utmost knowledge, this is the first report of the presence of arabinose in EPSs obtained from *B. licheniformis* which may be attributed to the association of bacteria to seaweed (Chi & Zhao, 2003). The monosaccharide composition of present EPS appears to be variably composed from that of the EPS produced by a number of marine bacteria like *Flavobacterium* and *Pseudoalteromonas* sp. (Mancuso-Nichols, Garon, Bowman, Raguenes, & Guezennec, 2004). The monosaccharide composition as determined in the present study was found contrast to most of the bacterial and cyanobacterial EPSs reported till date (Rainer, Venzke, & Blaschek, 2007) and thus it is novel so far.

3.5. UV–Vis, FT-IR and ^{1}H NMR analysis

UV–Vis spectroscopy analysis showed that the maximum wavelength area of absorption spectra was 200–230 nm due to n–σ^* and/or π–π^* transitions, which characterizes functional groups like amine, carboxyl, carbonyl and ester (Yun & Park, 2003) (Fig. S3). Moreover, a shoulder was observed around 260–280 nm which is commonly attributed to π–π^* electron transitions in aromatic and poly-aromatic compounds found in most conjugated molecules including proteins (Jia et al., 2007).

FT-IR analysis showed a broadly stretched intense peak at around 3428 cm^{-1} characteristic of hydroxyl groups and a weak C–H band at around 2928 cm^{-1} (Fig. 3A). The relatively strong absorption peak at around 1646 cm^{-1} indicated the characteristic IR absorption of polysaccharides (Bremer & Geesey, 1991). A symmetrical stretched peak near 1380 cm^{-1} indicated the presence of carboxyl groups. A comparison of functional groups revealed that EPS contained variable functional groups and were more complex than other EPSs previously reported (Chi & Zhao, 2003). The prominent absorption observed at 1646 cm^{-1} was attributed to the stretching vibration of C=O and C–N. The absorption at 1121 cm^{-1} could be attributed to the presence of sulfate groups as S=O and C–O–S (Parikh & Madamwar, 2006). Specifically, the peaks at 872 cm^{-1} ascertain the presence of glycosidic linkage bonds. The FT-IR spectra of the polymer showed the presence of carboxyl groups, which may presumably serve as binding sites for divalent cations (Bramhachari et al., 2007). In addition, the presence of both hydroxyl and carboxyl groups could be responsible for the high mucous polysaccharide formation thus, imparting emulsification potential (Kumar, Mody, & Jha, 2007).

The ^{1}H NMR spectrum showed seventeen anomeric signals for the EPS produced by *B. licheniformis* (Fig. 3B) depicting complex and heterogeneous nature of EPS. The signal at δ 2.49 ppm was exclusively detected in EPS of *B. licheniformis* indicating the presence of succinyl group. The complex nature of the biopolymer produced by *B. licheniformis* was further concluded by convergence of signals in the region of δ 3.2–3.9 ppm. The signals at δ 1.0–1.258 ppm arouse from the methyl protons of the 6-deoxy sugars (Kumar, Joo, Choi, Koo, & Changa, 2004).

3.6. Particle size distribution, energy dispersive X-ray spectroscopy (EDS or EDX) and AFM

EPS constituted of varied particle sizes from 5.274 (d 0.1) to 68.447 (d 0.9) μm with an average size of 24.977 μm (d 0.5) and 0.63771 m^2 g^{-1} specific surface areas (Fig. S4). EDX relies on the investigation of sample through interactions between electromagnetic radiation and matter, analyzing X-rays emitted by the matter in response to be hitted with charged particles (Goldstein et al., 2003). Elemental quantitative analysis done by EDX revealed the weight and atomic percentage of seven elements present in EPSs (Table 1). To the best of our knowledge this is first EDX study for EPSs of marine bacteria. The sulfate is present as a functional group in the EPS which confer its anionic character in the marine environment (Nielsen & Jahn, 1999). The distribution of cations such as Na, and Ca in the EPS detected in the EDX suggested their binding to the negative charges of the sulfate groups resulted in the greater availability of these elements to seaweeds essential for their growth and development. In addition, in a natural marine envi-

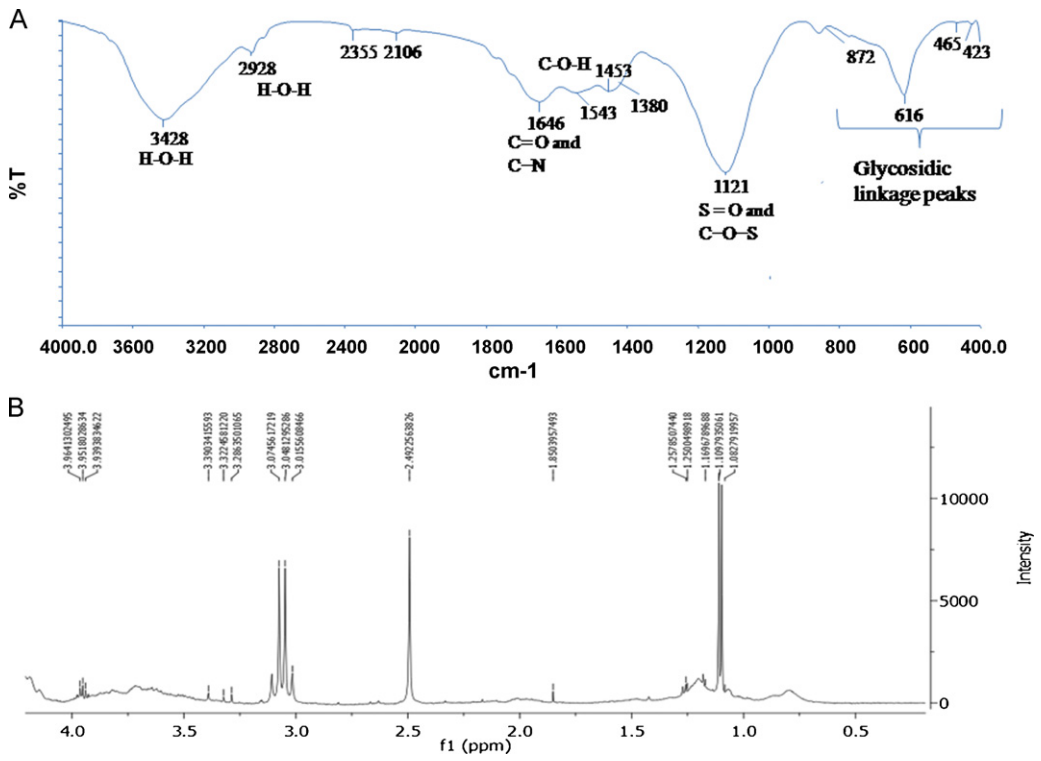

Fig. 3. FT-IR (A) and ^{1}H NMR (B) analysis of EPSs production by *B. licheniformis*.

Table 1
Elemental EDX micro analysis of EPSs obtained from EPSs of *B. Licheniformis*. Data are expressed with weight and atomic percents.

Element	Standard	Weight%	Atomic%
C	$CaCO_3$	38.48	46. 49
O	SiO_2	55.71	50. 53
Na	Albite	2.34	1.48
P	GaP	0.50	0.24
S	FeS_2	1.47	0.67
Ca	Wollastonite	0.25	0.09
Cl	KCl	1.24	0.51
Total		100	

Number of iterations = 3.

ronment, the nutrients can interact with EPS in order to increase the rate of elements uptake and concentrate the dissolved organic compounds, making them available to support microbial growth. Availability of phosphate in the seawater increase the growth of the phytoplankton *Cylindrotheca fusiformis* and it might increase the primary production in the ocean (Guerrini, Mazzotti, Boni, & Pistocchi, 1998).

Properties of EPS chain can be determined by measuring parameters like contour lengths, persistence lengths and end-to-end distances of the chain using AFM. The 3D structure of the EPS of *B. licheniformis* can present with AFM in live condition than scanning electron microscope. The size of different particle within EPS was showed the height distribution profiles of the surface roughness (Fig. 4 and Fig. S5). Roughness average was 191 nm and histogram of the AFM showed the distribution profile of particle of EPS on the cover slide.

3.7. X-ray diffraction (XRD) analysis

X-ray diffraction (XRD) is a very powerful analytical technique widely used for phase identification of materials. The XRD profile

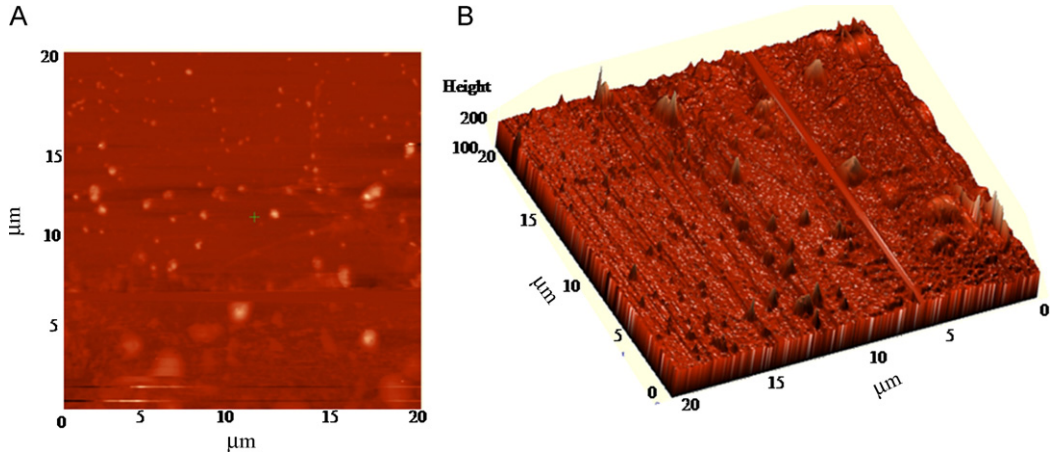

Fig. 4. AFM analysis [two (A) and three dimensional views (B)] of EPSs and EPSs distribution on the cover slip.

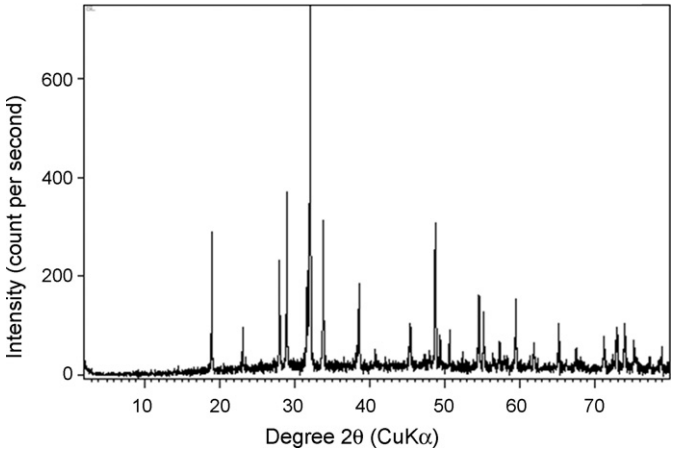

Fig. 5. XRD profile of EPSs isolated from *B. licheniformis*.

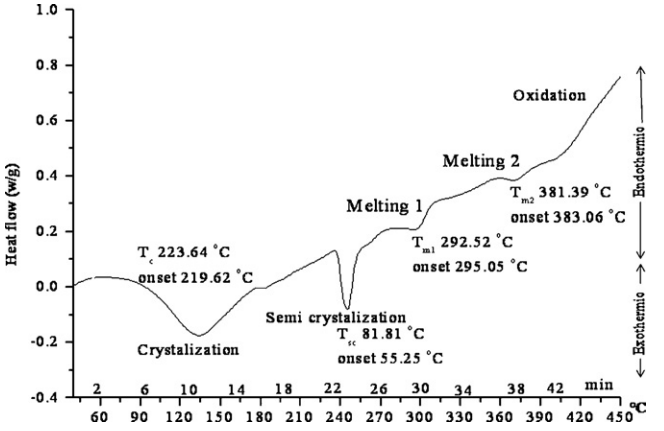

Fig. 7. DSC thermogram of EPSs obtained from *B. licheniformis* at heating rate of 10 °C.

of EPS obtained from *B. licheniformis* exhibited the characteristic diffraction peaks at 32.1 and 49.4° with inter planar spacing (*d*-spacing) 2.786 and 1.680 Å, respectively (Fig. 5 and Fig. S6). Powder XRD pattern revealed that EPS is amorphous in nature with CI_{xrd} 0.397 crystallinity index. It is difficult to interpret broad amorphous peaks of several amorphous EPS in X-ray scattering profile (Shimazu, Miyazaki, & Ikeda, 2000) while easy to interpret narrow crystalline peaks and therefore the ratio between sharp narrow diffraction peaks and broad peak was used to calculate the amount of crystallinity in the EPS. The 39.7% crystalline domains act as a reinforcing grid and improve the performance over a wide range of temperature as observed in TG and DSC analysis.

3.8. TG and DSC analysis

TGA was carried out dynamically between weight loss vs temperatures and experimental result shown in Fig. 6. TGA showed that degradation of EPS obtained from *B. licheniformis* takes place in two steps while EPSs of *Bacillus* sp. I-450 showed the degradation in three steps (Kumar et al., 2004). Seven percent of total EPSs weight loss from 30 to 120 °C was recorded due to moisture content, thereafter second phase of degradation (59.6%) was observed with maximum loss at ≥330 °C. High level of carboxyl group in the EPSs increased the degradation of the first phase as carboxyl group is bound to more water molecules (Kumar et al., 2004). The total weight loss of EPS occurred after 330 °C, however

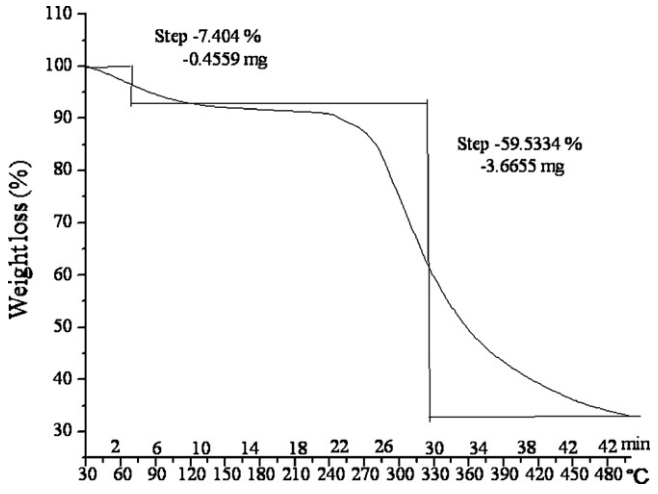

Fig. 6. TG thermogram of EPSs obtained from *B. licheniformis* at heating rate of 10 °C.

EPS of the *Bacillus* sp. CP912 (Yun & Park, 2003) showed pyrolysis temperature at 284.58 °C. With the increase in temperature amorphous solid becomes less viscous and at a meticulous temperature the molecules gain enough freedom of motion to spontaneously arrange themselves into a crystalline state which is crystallization temperature. This transition is an exothermic process and DSC analysis showed a significant thermal transition of EPS into a crystalline state. DSC thermogram showed two distinct exothermic peaks of EPS with crystallization temperature (T_c) 223.64 °C (onset temperature 219.62 °C), semi crystallization temperature (T_{sc}) 81.81 °C (onset temperature 55.25 °C) accompanied with 538.51 and 128.40 mJ latent energy, respectively (Fig. 7). The melting peaks were found at 295.05 °C (onset temperature 292.52 °C) with 61.79 mJ latent energy for T_{m1} and 383.06 °C (onset temperature 381.39 °C) with 23.36 mJ latent energy for T_{m2}. The present study of DSC thermogram is different from our previous report (Mishra et al., 2011) in which EPS showed one melting peak of an endothermic transition and crystallization peaks of an exothermic transition. The activation energy (*n*th order of reaction) of exothermic transitions was 68.23 ± 0.17 (T_c) and 549.30 ± 3.45 kJ mol^{-1} (T_{sc}), it was found quite higher from 245.77 ± 1.32 (T_{m1}) and 667.31 ± 3.43 (T_{m2}) kJ mol^{-1} for endothermic transition. This phenomenon may be to the different molecular mass structures of the EPS as detected with GPC. The melting point and endothermic calories of the EPS isolated from marine *Bacillus* sp. CP912 was found to be 128.7 °C and 50.864 kcal mol^{-1} and revealed that EPS of *B. licheniformis* is more stable than earlier reports (Yun & Park, 2003). In coherence with XRD, approximately equal crystalline index (CI_{DSC} 0.40) was observed for EPS from DSC thermogram and same variation may be because of uncertainties in placing base line for area integration (Khanna & Kuhn, 1997).

3.9. MALDI TOF-TOF mass spectroscopy

MALDI TOF-TOF MS is a convenient method for rapid and sensitive structural analysis of oligosaccharides (Guerrini et al., 1998). The MALDI TOF-TOF MS was optimized for EPS and fragmentation peaks were detected with positive ion mode (Mishra et al., 2011). MALDI TOF-TOF MS of EPS (Fig. S7) represented a series of masses *m*/*z* 175.0767, 175.1204, 197.1340, 197.1543 and 253.1514 in low range mode which corresponded to de-protonated hexose sugar and hexose sugar with inorganic and organic groups as identified with spectroscopic analysis (FT-IR, ^{1}H NMR and UV–Vis) and EDX. Besides this, the mass fragment of *m*/*z* 329.2139 was also observed in positive ion mid range mode, corresponding to the masses of two pentose sugars. The positive ion reflector mode exhibited low mass peaks *m*/*z* 609.3466 (2 hexose and 2 pentose sugars), 684.3428,

691.9866, 738.4248, 746.5306, 749.3351 and 767.6293 corresponding to a tetrasaccharide (4 hexose sugars) and 839.5795, 853.4269, 875.5742, 881.4112 and 897.5235 corresponding to a pentasaccharide. The peaks of 911.4109, 917.5286 and 947.4280 revealed the presence of hexasaccharide chain of 4 hexoses and 2 pentoses while the peaks of 964.4944, 972.6881, 986.0231, and 996.6495 corresponded to hexasaccharide chain of 6 hexose sugars. The higher numbers of mass peaks, m/z from 1015.6401 to 1539.0313 revealed polysaccharides consisting of different ratios of pentose and hexose sugars associated with different ions (S, Na, P, Ca, Cl, C and O), as detected by spectroscopic and EDX analysis. It may be the first MALDI TOF-TOF MS report of EPSs of bacterial origin so far however; Gauri, Mandal, Mondal, Dey, and Pati (2009) recently reported MALDI-TOF MS for the EPS obtained from *Azotobacter* sp. SSB81. Further, this analysis also confirmed the presence of galactose, glucose, mannose and arabinose in different combinations as revealed by GC–MS analysis. Though the mass spectroscopy did not distinguish diastereomers but it indicated the number of sugar moiety in an oligomer.

4. Conclusion

The extracellular polymeric substances are of immense biotechnological and industrial importance. In the present study, the EPS obtained from *B. licheniformis* was characterized with the help of advanced analytical methods. AFM, MALDI-TOF-TOF MS, XRD, EDX and DSC analysis are the first reports for EPS obtained from marine bacterial origin. The ^{1}H NMR, FT-IR and UV–Vis spectroscopic analyses revealed the complex and heterogeneous nature of EPS, TGA highlighted its high thermal stability (330 °C) while DSC and XRD analysis depicted its amorphous nature with crystalline index (CI_{DSC} 0.40). XRD profile and interplanar spacing (d-spacing) is the basic characteristic of a polymer useful to compare or study the nature of EPS isolated from different sources in future. Galactose, glucose, mannose and arabinose were the monosaccharides detected by GC–MS analysis and MALDI-TOF-TOF MS further aided in unraveling oligosaccharide composition. The EPS may allow further exploration of *B. licheniformis* making them promising candidates for their commercial exploitation. The emulsification activity revealed that it can be exploited for environmental bioremediation. Further, the characterization of the EPS might be of helpful for the seaweed bacterial interaction to find out the molecules that enhance the growth of seaweeds for future research.

Acknowledgements

The financial support received from the Council of Scientific and Industrial Research (NWP-018), New Delhi is gratefully acknowledged. The authors PK (CSIR-JRF), RPS (Project-SRF) and MKS (Project-JRF) gratefully acknowledge the CSIR, New Delhi for their fellowship.

Appendix A. Supplementary data

Supplementary data associated with this article can be found, in the online version, at doi:10.1016/j.carbpol.2010.12.061.

References

Arias, S., Moral, A. D., Ferrer, M. R., Tallon, R., Quesada, E., & Bejar, V. (2003). Mauran, an exopolysaccharide produced by the halophilic bacterium *Halomonas maura*, with a novel composition and interesting properties for biotechnology. *Extremophiles*, *7*, 319–326.

Bermudez, J., Rosales, N., Loreto, C., Briceno, B., & Morales, E. (2004). Exopolysaccharide, pigment and protein production by the marine microalga *Chroomonas* sp. in semicontinuous cultures. *World Journal of Microbiology and Biotechnology*, *20*, 179–183.

Bhaskar, P. V., & Bhosle, N. B. (2005). Microbial extracellular polymeric substances in marine biogeochemical processes. *Current Science*, *88*, 1.

Bradford, M. M. (1976). A rapid and sensitive method for the quantification of microgram quantities of protein utilizing the principle protein–dye binding. *Analytical Biochemistry*, *72*, 248–254.

Bramhachari, P. V., Kishor, P. B. K., Devi, R. R., Kumar, R., Rao, B. R., & Dubey, S. K. (2007). Isolation and characterization of mucous exopolysaccharide (EPS) produced by *Vibrio furnissii* strain VB0S3. *Journal of Microbiology and Biotechnology*, *17*, 44–51.

Bremer, P. J., & Geesey, G. G. (1991). An evaluation of biofilms development utilizing non-destructive attenuated total reflectance Fourier transform infrared spectroscopy. *Biofouling*, *3*, 89–100.

Chi, Z., Su, C. D., & Lu, W. D. (2007). A new exopolysaccharide produced by marine *Cyanothece* sp. 113. *Bioresource Technology*, *98*, 1329–1332.

Chi, Z., & Zhao, S. (2003). Optimization of medium and cultivation conditions for pullulan production by new pullulan-producing yeast. *Enzyme and Microbial Technology*, *33*, 206–211.

Costerton, J. W. (1999). The role of bacterial exopolysaccharides in nature and disease. *Journal of the Indian Microbiology and Biotechnology*, *22*, 551–563.

Decho, A. W. (1990). Microbial exopolymer secretion ocean environment, their roles in food webs and marine processes. *Marine Biology*, *28*, 73–153.

Dodgson, K. S., & Price, R. G. (1963). A note on the determination of the ester sulfate content of sulfated polysaccharides. *Journal of Biochemistry*, *84*, 350–356.

Duan, X., Chi, Z., Wang, L., & Wang, X. (2008). Influence of different sugars on pullulan production and activities of α-phosphoglucose mutase, UDPG-pyrophosphorylase and glucosyltransferase involved in pullulan synthesis in *Aureobasidium pullulans* Y68. *Carbohydrate Polymers*, *73*, 587–593.

Freitas, F., Alves, V. D., Pais, J., Costa, N., Oliveira, C., Mafra, L., et al. (2009). Characterization of an extracellular polysaccharide produced by a *Pseudomonas* strain grown on glycerol. *Bioresource Technology*, *100*, 859–865.

Gauri, S. S., Mandal, S. M., Mondal, K. C., Dey, S., & Pati, B. R. (2009). Enhanced production and partial characterization of an extracellular polysaccharide from newly isolated *Azotobacter* sp. SSB81. *Bioresource Technology*, *100*, 4240–4243.

Goldstein, J., Newbury, D. E., Joy, D. C., Lyman, C. E., Echlin, P., Lifshin, E., et al. (2003). *Scanning electron microscopy and X-ray micro analysis* (3rd ed.). Dordrecht, Netherland: Springer.

Grabar, K. C., Freeman, R. G., Hommer, M. B., & Natan, M. J. (1995). Preparation and characterization of Au colloid monolayers. *Analytical Chemistry*, *67*(*4*), 735–743.

Guerrini, F., Mazzotti, A., Boni, L., & Pistocchi, R. (1998). Bacterial–algal interaction in polysaccharide production. *Aquatic Microbial Ecology*, *15*, 247–253.

Jia, S., Yu, Y., Lin, H., & Dai, Y. (2007). Characterization of extracellular polysaccharides from *Nostoc flagelliforme* cells in liquid suspension culture. *Biotechnology and Bioprocess Engineering*, *12*, 271–275.

Khanna, Y. P., & Kuhn, W. P. (1997). Measurement of crystalline index in nylons by DSC: Complexities and recommendations. *Journal of Polymer Science Part B: Polymer Physics*, *35*, 2219–2231.

Kumar, A. S., Mody, K., & Jha, B. (2007). Evaluation of biosurfactant/bioemulsifier production by a marine bacterium. *Bulletin of Environment Contamination and Toxicology*, *79*, 617–621.

Kumar, C. G., Joo, H. S., Choi, J. W., Koo, Y. M., & Changa, C. S. (2004). Purification and characterization of an extracellular polysaccharide from haloalkalophilic *Bacillus* sp. I-450. *Enzyme and Microbial Technology*, *34*, 673–681.

Mancuso-Nichols, C. A., Garon, S., Bowman, J. P., Raguenes, G., & Guezennec, J. (2004). Production of exopolysaccharides by Antarctic marine bacterial isolates. *Journal of Applied Microbiology*, *96*, 1057–1066.

Manzoni, M., & Rollini, M. (2001). Isolation and characterization of the exopolysaccharide produced by *Daedalea quercina*. *Biotechnology Letters*, *23*, 1491–1497.

Marshall, K., Joint, I., Callow, M. E., & Callow, J. A. (2006). Effect of marine bacterial isolates on the growth and morphology of axenic plantlets of the green alga *Ulva linza*. *Microbial Ecology*, *52*, 302–310.

Mata, J. A., Bejar, V., Llamas, I., Arias, S., Bressollier, P., Tallon, R., et al. (2006). Exopolysaccharides produced by the recently described bacteria *Halomonas ventosae* and *Halomonas anticariensis*. *Research in Microbiology*, *157*, 827–835.

Maugeri, T. L., Gugliandolo, C., Caccamo, D., Panico, A., Lama, L., Gambacorta, A., et al. (2002). A halophilic thermotolerant *Bacillus* isolated from a marine hot spring able to produce a new exopolysaccharide. *Biotechnology Letters*, *24*, 515–519.

Mishra, A., & Jha, B. (2009). Isolation and characterization of extracellular polymeric substances from micro-algae *Dunaliella salina* under salt stress. *Bioresource Technology*, *100*, 3382–3386.

Mishra, A., Kavita, K., & Jha, B. (2011). Characterization of extracellular polymeric substances produced by micro-algae *Dunaliella salina*. *Carbohydrate Polymers*, *82*, 852–857.

Nielsen, P. H., & Jahn, A. (1999). Microbial extracellular polymeric substances: Characterization, structure and function. In J. Wingender, T. R. Neu, & H. C. Flemming (Eds.), *Extraction of EPS* (pp. 50–72). Berlin, Germany: Springer-Verlag.

Parikh, A., & Madamwar, D. (2006). Partial characterization of extracellular polysaccharides from cyanobacteria. *Bioresource Technology*, *97*, 1822–1827.

Rainer, B. V., Venzke, K., & Blaschek, W. (2007). Structural investigation of a polysaccharide released by the cyanobacterium *Nostoc insulare*. *Journal of Applied Phycology*, *19*, 255–262.

Ricou, P., Pinel, E., & Juhasz, N. (2005). Temperature experiments for improved accuracy in the calculation of polyamide-11 crystallinity by X-ray diffraction. *Advances in X-ray analysis*,. International Centre for Diffraction Data

Rougeaux, H., Talaga, P., Carlson, R. W., & Guezennec, J. (1998). Structural studies of an exopolysaccharide produced by *Alteromonas macleodii* sub sp. *fijiensis* originating from a deep-sea hydrothermal vent. *Carbohydrate Research*, *312*, 53–59.

Shimazu, A., Miyazaki, T., & Ikeda, K. (2000). Interpretation of *d*-spacing determined by wide angle X-ray scattering in 6 FDA-based polyimide by molecular modelling. *Journal of Membrane Science*, *166*, 113–118.

Siddhanta, A. K., Goswami, A. M., Shanmugam, M., Mody, K. H., Ramavat, B. K., & Maihr, O. P. (2001). Water soluble polysaccharide of marine algae species *Ulva* (Ulvales, Chlorophyta) of Indian waters. *Indian Journal of Marine Science*, *30*, 166–172.

Singh, R. P., Mantri, V. A., Reddy, C. R. K., & Jha, B. (2011). Isolation of seaweed associated bacteria and their morphogenesis inducing capability in axenic cultures of the green alga *Ulva fasciata*. *Aquatic Biology*, doi:10.3354/ab00312.

Tatewaki, M., Provasoli, L., & Pintner, I. J. (1983). Morphogenesis of *Monostroma oxyspermum* (Kutz) Doty (chlorophyceae) in axenic culture, especially in bioalgal culture. *Journal of Phycology*, *19*, 409–416.

Wang, Y., Zhang, M., Ruan, D., Shashkov, A. S., Kilcoyne, M., Savage, A. V., et al. (2004). Chemical components and molecular mass of six polysaccharides isolated from the sclerotium of *Poria cocos*. *Carbohydrate Research*, *339*, 327–334.

Yemm, E. W., & Willis, A. J. (1954). The estimation of carbohydrates in plant extracts by anthrone. *Journal of Biochemistry*, *57*, 508–514.

Yun, U. J., & Park, H. D. (2003). Physical properties of an extracellular polysaccharide produced by *Bacillus* sp. CP912. *Letters in Applied Microbiology*, *36*, 282–287.

Zhenming, C., & Yan, F. (2005). Exopolysaccharides from marine bacteria. *Journal of Ocean University China*, *4*, 67–74.

Zou, X., Sun, M., & Guo, X. (2006). Quantitative response of cell growth and polysaccharide biosynthesis by the medicinal mushroom *Phellinus linteus* to NaCl in the medium. *World Journal of Microbiology and Biotechnology*, *22*, 1129–1133.